Nonlinear phenomena in the quantum Hall effect

V. M. Pudalov and S. G. Semenchinskiĭ

All-Union Scientific-Research Institute of the Metrological Service
(Submitted 9 August 1983)
Zh. Eksp. Teor. Fiz. **86**, 1431–1445 (April 1984)

The shape of the plateau in Hall resistance ρ_{xy} and minima of the resistivity ρ_{xx} and their current and temperature dependences have been investigated experimentally on Si MIS's. The width of the ρ_{xy} plateau was found to decrease linearly with increase in current and temperature. The wings of the ρ_{xx} minimum have an exponential shape. The main cause of the deviation of ρ_{xx} from the quantized value h/Ne^2 could be established from the linear relationship found between ρ_{xx} and ρ_{xy} in the region of the plateau; this is the variation in the concentration of mobile carriers. A qualitative quasiclassical theory is proposed which is based on the concept of carrier localization at the potential fluctuations and which can explain most of the experimental results.

1. INTRODUCTION

As is well known, a macroscopic quantum effect arises in a two-dimensional (2D) layer of carriers placed in a transverse magnetic field, which has received the name "quantum Hall effect" (QHE) in the literature;[1] the resistivity tensor of the two-dimensional layer then takes the form[1,2]

$$\rho_{l,m}=h/Ne^2, \quad l\neq m, \tag{1}$$

$$\rho_{l,m}\approx 0, \quad l=m, \tag{2}$$

where $N=1, 2, \ldots$ are integers. Equations (1) and (2) are satisfied in a number of ranges of carrier concentration n (for fixed H) or in a number of H ranges (for fixed n), and the accuracy with which Eq. (1) is satisfied in $\sim 10^{-7}$.[3]

In existing theoretical models the explanation of the QHE is based on the assumption of bound electron states in the 2D layer, which cannot carry current[4] and are situated in the region of the energy gap in the spectrum of mobile states.[4,5] As possible mechanisms for bound states to arise, Wigner crystallization,[6] charge density waves,[7] tunneling of carriers across the potential barrier at the heterojunction[8] and localization of carriers at potential fluctuations[9,5] have been considered.

All the theoretical models mentioned lead to Eqs. (1) and (2), so that the choice of one theory or another can only be made by comparing the departures from Eqs. (1) and (2), which arise in real materials, with conclusions from the theory obtained in the next approximation. The present authors had as their aims an experimental study of the departures of ρ_{xx} and $\delta\rho_{xy}$ from the ideal relations of Eqs. (1) and (2), the establishment of the relationships in the dependences of ρ_{xx} and $\delta\rho_{xy}$ on temperature and measuring current and comparison of them with conclusions of the theory. Preliminary experiments[10] indicated that the corrections to Eqs. (1) and (2) are appreciably nonlinear, i.e., they depend on current under all measuring conditions. All the experimental results given below, unless specially noted to the contrary, refer to the plateau region with $N=4$.

2. EXPERIMENTS

2.1 Specimens

The metal-insulator-semiconductor (MIS) structures[11] studied were prepared on (100) surfaces of p-type silicon. The

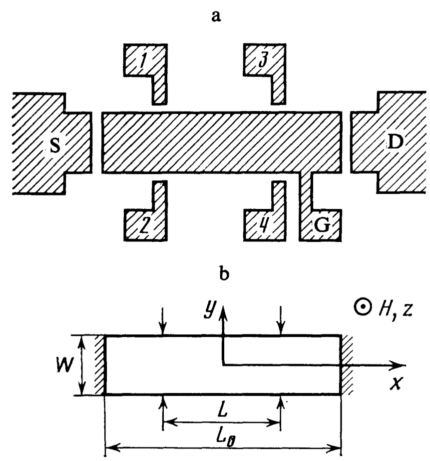

FIG. 1. a) Appearance in the plane of the MIS structure (metallic regions are shaded); orientations of the measuring current J_x, of Hall field E_y and of the magnetic field H relative to the specimen. Notation of the contacts: S-source, D-drain, G-gate, 1 to 4-potential contacts.

appearance in the plane of the structure is shown in Fig. 1 with 4 potential contacts to the 2D layer of carriers. The carrier concentration in the 2D layer is controlled by applying a voltage V_g to the gate relative to one of the electrodes, the source or the drain.[11] The average values of the components of the resistivity tensor can be measured by the voltage drop along the current V_x and perpendicular to it V_y:

$$\langle\rho_{xy}\rangle=\frac{V_y}{J_x}=\frac{\int_{-W/2}^{W/2} j_x\rho_{xy}\,dy}{\int_{-W/2}^{W/2} j_x\,dy}, \tag{3}$$

$$\langle\rho_{xx}\rangle=\frac{W}{L}\frac{V_x}{J_x}, \tag{4}$$

where J_x and j_x are the total current and the current density across the 2D layer (it is assumed that $j_y=0$, i.e., the Hall contacts are open circuited). Two types of specimen were studied: one with small channel area ($L_0=500$, $L=150$, $W=50\,\mu$m), thickness of insulator $d_{SiO_2}=2000$ Å and mobility at the maximum $\mu^{max}\approx 1\times 10^4$ cm^2 V^{-1} s^{-1};[12] and the

 0038-5646/84/040838-09$04.00

other with large channel area ($L_0 = 1200, L = 400, W = 400$ μm) insulator thickness $d_{SiO_2} = 1300$ Å and mobility $\mu^{max} \approx 1.6 \times 10^4$ cm^2 V^{-1} s^{-1}. A potentiometer circuit[13] was used to measure the voltages V_y and V_x; a comparison resistor was included in series with the channel in the current transmission circuit, for measuring V_y. The specimens were contained in a vacuum-tight container filled with ^{3}He gas, which served to make thermal contact with the liquid ^{3}He bath. The specimen temperature was controlled by pumping off ^{3}He vapor. The magnetic field direction coincided with the normal to the plane of the 2D layer, i.e., to the z direction (Fig. 1).

2.2 Achieving an equilibrium potential distribution in the 2D layer

The resistivity of the Si substrate is very high at helium temperatures, $\gtrsim 10^{14}$ Ω·cm; the time for establishing an equilibrium charge concentration in it is then many hours. At helium temperatures the rate of filling traps near the Si/SiO_2 boundary is also exponentially small. All this can lead to a nonequilibrium potential distribution arising and to an anomalously large amplitude of its fluctuations. The value of the mobility is then lowered somewhat, the shape of the ρ_{xy} plateau is strongly deformed and the value of ρ_{xx} at the minima increases by several orders of magnitude.[5,14]

The equilibrium state can be established in such cases by heating the specimen up to a temperature $T \gtrsim 77$ K (at which conductivity appears in the substrate) or by illuminating the specimen with infrared radiation.[14]

In the present work we have estimated the magnitudes of the possible corrections to Eq. (1), by studying the departures of $\delta\rho_{xy}$ and ρ_{xx} from Eqs. (1) and (2) on the wings of the plateau (the shape of the plateau). It is obvious that the establishment of the equilibrium state is an essential condition for studying the shape of the plateau. As can be seen from Fig. 2, ρ_{xy} in the middle section of the plateau is constant in the equilibrium state to an accuracy up to $|\delta\rho_{xy}/\rho_{xy}| < 10^{-6}$, and the dependences of the shape on various parameters are repeated qualitatively from experiment to experiment and also for different specimens.

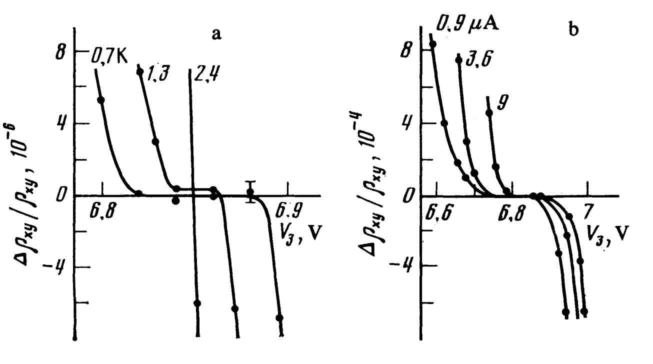

FIG. 2. Shape of the $\rho_{xy}(V_g)$ plateau for one and the same specimen in the equilibrium state: as a function of temperature at $J_x = 9$ μA (a) and of current at $T = 0.7$ K (b).

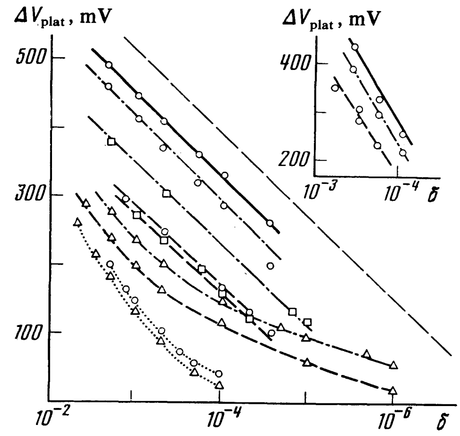

FIG. 3. Dependence of the width ΔV_{plat} of the ρ_{xy} plateau ($N = 4$) on the modulus of the given relative deviation δ: ○—$J_x = 0.9$ μA, □—3.6 μA, △—9 μA; full lines are for $T = 0.4$ K, dashed dot—0.68 K, dashed line—1.3 K, dotted ~2.36 K. The thin dashed line without experimental points is an extrapolation to $J_x = 0$, $T = 0$.

2.3 Shape of the plateau

We took as the quantitative characteristic of the shape of the plateau, the width of the voltage range on the gate ΔV_{plat}, measured at the level of a fixed relative departure δ of the Hall resistivity ρ_{xy} from the reference value for which was chosen the value of ρ_{xy} at the center of the plateau at $T = 0.7$ K, $J_x = 9$ μA. The dependence of plateau width on δ for different currents and temperatures is shown in Fig. 3. The family of curves in the figure are drawn for a specimen with large channel area; the results in the inset are for specimens with small channel area.

Over a fairly wide range of departures $\delta = 10^{-3}$–10^{-4}, currents $J_x = 0.1$–9 μA and of temperatures $T = 0.4$–2.4 K, the $\Delta V_{plat}(\delta)$ dependence is of logarithmic form with the shape of the corresponding straight lines almost independent of current and temperature, as can be seen from Fig. 3. The exception consists of the region of high temperatures $T \approx 2.4$ K and large currents $J_x \geqslant 9$ μA, where the logarithmic dependence, if it exists, does so in an appreciably smaller range of δ. Under these conditions the width of the plateau decreases approximately linearly on increasing current or temperature (Fig. 4).

The results of the experiment are described by an empirical relation between the width of the plateau, temperature, current and relative departure of the resistivity (at $H = 80$ kOe, $T < T^c$, $J_x < J^c$):

$$\Delta V_{plat} \approx 10(T^c - T)(J^c - J_x) + 115 \lg \delta + B. \qquad (5)$$

Here ΔV_{plat} is in mV, $T^c \approx 2.5$ K, $J^c \approx 15.3$ μA, $B = 480$ mV. Such a form of dependence would be difficult to explain if the departure $\delta\rho_{xy}$ at the wings of the plateau were only determined by an increase in the dissipative component of the resistivity tensor. In fact, by using the empirical relation $\delta\rho_{xy} \infty \rho_{xx}$[10] (see also §2.4) and assuming a temperature dependence $\rho_{xx} \propto \exp(-T^{-\beta})$ (Ref. 15), we obtain $\Delta V_{plat} = A + T^{\beta} \ln\delta$ (where A is a constant and $\beta = \frac{1}{3}, \frac{1}{2}$ or 1, depending on the conductivity mechanism) as distinct from Eq. (5).

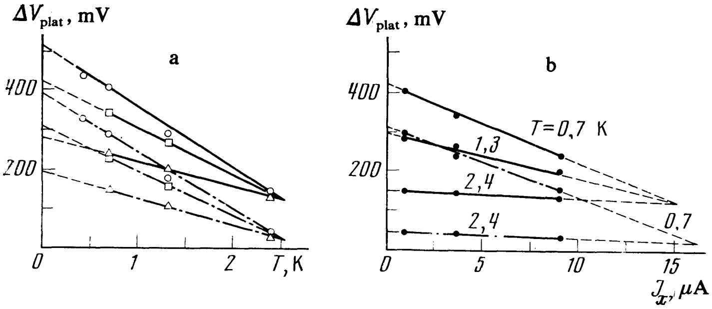

FIG. 4. Width of the ρ_{xy} ($N=4$) plateau, ΔV_{plat}, measured at the level of a given relative departure δ from the value $h/4e^2$: a) as a function of temperature ○—$J_x=0.9\,\mu$A, □—$3.6\,\mu$A, △—$9\,\mu$A), b) as a function of current. Full lines $|\delta|=10^{-3}$, dashed lines $|\delta|=10^{-4}$.

Because of the rapid growth in experimental errors (Fig. 3) in the region $\delta=10^{-5}$–10^{-6}, only an approximate linear extrapolation corresponding to Eq. (5) can be carried out to the center of the plateau ($\Delta V_{\text{plat}}\to 0$). As can be seen from Fig. 3 and Eq. (5), such an extrapolation gives an upper estimate to the limiting departure from the ideal value of Eq. (1) for the center of the plateau: $\delta\leqslant 2\times 10^{-7}$ for $J_x=0.9\,\mu$A, $T=0.4$ K and $\delta\leqslant 3\times 10^{-8}$ for $J_x=0$ and $T=0$ under the experimental conditions described.

2.4. Relation between the resistivity tensor components. The shape of the ρ_{xx} minimum

It is natural to look for corrections $\delta\rho_{xy}$ in the form of a polynomial in powers of the small parameter (ρ_{xx}/ρ_{xy}) (Ref. 5), i.e., to look for a relation between $\delta\rho_{xy}$ and ρ_{xx}. The question of the connection between $\delta\rho_{xy}$ and ρ_{xx} from the experimental point of view is in need of detailed investigation. The region of carrier concentrations n near the center of the plateau ^0V_g corresponds to a position of the Fermi level $\mathscr{E}_F$ between two neighboring Landau levels, where the density of states $D(\mathscr{E}_F)$ is close to zero. Since the screening radius[11]

$$r_0=[(2\pi e^2/\varkappa)D(\mathscr{E}_F)]^{-1}$$

is then a maximum ($\varkappa=11.8$ is the dielectric susceptibility of Si), then the potential fluctuations in the two-dimensional layer are weakly screened and, consequently, the state of the specimen is the least uniform. The values of ρ_{xx} and ρ_{xy}, statistically averaged for one and the same section of the specimen must therefore enter into the relation sought.

In a specimen of rectangular geometry (Fig. 1), the measured value of ρ_{xx} characterizes a section between two potential contacts along the channel, while ρ_{xy} corresponds to a transverse section of the channel. The possibility of establishing a relation between ρ_{xx} and $\delta\rho_{xy}$ in the central region of the ρ_{xy} plateau is thus not obvious. The absence of a unique connection between ρ_{xy} and ρ_{xx} at the center of the plateau is also illustrated by the following simple fact: there exists for any $\rho_{xy}(V_g)$ dependence in the region of the plateau at least one point at which ρ_{xy} is exactly equal to h/Ne^2, i.e., $\delta\rho_{xy}=0$. At the same time a departure from ρ_{xx} having a value zero is known to be observed experimentally.

Measurements were carried out in a carrier concentration range more favorable from the experimental point of view, on the wings of the ρ_{xy} plateau. The density of states near the Fermi level $D(\mathscr{E}_F)$ in this region is different from zero and the state of the specimen can be considered uniform.[10] An experiment carried out on specimens with large channel area in the temperature range 0.4–2.4 K and currents 0.9–9 μA at $H=80$ kOe[16] showed that there is a linear relation between ρ_{xx} and $\delta\rho_{xy}$ in the range $10^{-5}<|\delta\rho_{xy}/\rho_{xy}|<10^{-2}$:

$$\delta\rho_{xy}/\rho_{xy}=\alpha_1(\rho_{xx}/\rho_{xy})\ \text{sign}\ (^0V_g-V_g), \tag{6}$$

where the coefficient $\alpha_1\approx 0.3\pm 0.1$ is practically independent of temperature and current. It also follows from the measurements[16] that the wings of the minimum of ρ_{xx} over a fairly wide range $10^{-5}(\rho_{xx}/\rho_{xy})<10^{-2}$ are of exponential shape:

$$\rho_{xx}\propto A\exp\left[|V_g-{}^0V_g|B\right], \tag{7}$$

with the curvature of the electron slope different from the hole slope: $B_e<B_h$. There is also a similar asymmetry of the electron and hole wings in the $\delta\rho_{xy}(V_g)$ dependence. We averaged the shape of the electron and hole wings in the analysis of the shape of the plateau in §2.3 by choosing the simplest parameter for the shape ΔV_{plat}.

3. QUALITATIVE QUASICLASSICAL QHE THEORY

Among the various reasons for bound states of carriers to arise, mentioned in the Introduction, the simplest and the one requiring least assumptions seemed to be the localization of carriers at potential fluctuations. This mechanism forms the basis of the model developed further to explain the experimental facts.

The behavior of the system of carriers depends on the nature of the fluctuations in the 2D layer. From the results of an experimental study of the Si/SiO_2 boundary[17] we distinguish two types of potential fluctuations: 1) short range (or of δ-form) with characteristic dimension $\mathscr{L}=14$–40 Å $<a_H\approx 70$ Å (where $a_H=(\hbar c/eH)^{1/2}$ is the magnetic length) and 2) long range with $\mathscr{L}\approx 200$–500 Å $\gg a_H$. Both types of fluctuations have an amplitude of the same order of magnitude: $\delta U\sim(\Delta/d_{SiO_2})U_s\sim 1$ meV where $\Delta=2$–8 Å is the root mean square height of the roughness of the surface,[17] U_s is the surface potential.[11] We note that potential fluctuations of dimensions larger than $\mathscr{L}_{\max}\approx d_{SiO_2}\sim 10^3$ Å are absent in the MIS system because of screening by the electrons of the metallic gate.

In the range of magnetic fields $H\gtrsim 70$ kOe in which the QHE is observed, the cyclotron splitting $\hbar\omega_c\gtrsim 7$ meV exceeds the amplitude of the potential fluctuations. Consequently, local systems of Landau levels can be introduced over all points of the 2D-space; the whole set of them over the xy plane forms a Landau subband of width 2Γ (Fig. 5). In

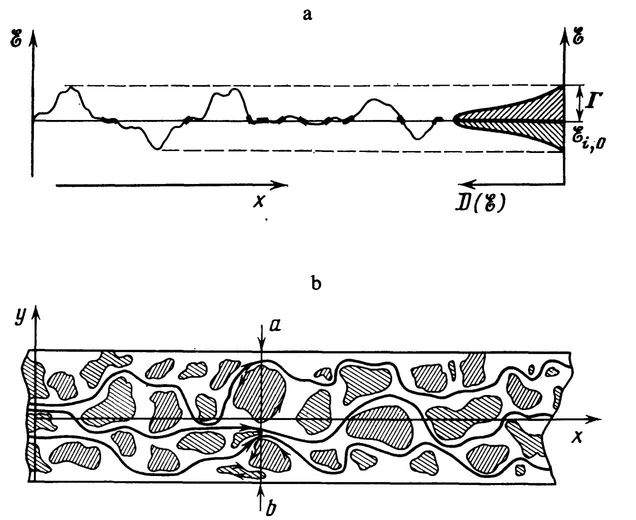

FIG. 5. a) Connection between the spatial potential variation $\mathscr{E}_i(x, y)$ of the 2D Landau level and the density of states in energy $D(\mathscr{E})$; b) schematic repesentation in the plane of infinite equipotentials of delocalized states at the percolation level and of finite equipotentials of bound states. The shaded regions of bound states are the "peaks" and "dips" of the potential variation. Regions of delocalized states are separated by the thick line. The arrows indicate the current directions in the a-b cross section.

what follows we shall everywhere ignore electron-electron interaction.

3.1 Linear Phenomena

3.1.1. Topological percolation properties of a two-dimensional potential

The division of states at one energy within a Landau level into mobile and localized is naturally connected with the division of the channel area into regions of localized and mobile states according to the potential fluctuation of the 2D-layer (Fig. 5). To each single-particle state corresponds its own equipotential. The dips in the potential are regions of electron localized states, the peaks are hole localized states[1)] since the equipotentials in these regions are finite. Infinite equipotentials (more exactly, extending over the whole specimen length) correspond to mobile states; their energy, by definition, corresponds to the percolation threshold at a 2D Landau level. Under conditions of symmetry in the potential fluctuations (peaks and dips) percolation in the 2D layer takes place, as is known,[18] just at the level separating equal concentrations of hole and electron regions, i.e., at the center of the Landau level $\mathscr{E}_{i,0}$.

In general, the possibility of using a classical description of carrier mobility in a 2D quantum level requires justification. This possibility is based on the fact that in the limit as $H\rightarrow\infty$ (more precisely $a_H \ll \mathscr{L}$) the energy eigenvalues $\mathscr{E}$ coincide with the classical equipotentials $U(x, y) = \mathscr{E}$ and the regions of space of area $\sim a_H^2$ where the wave function of a given state is different from zero goes over to a representative point on the classical equipotential trajectories.[19,20] For this reason a stricter quantum consideration[21,22] confirms the conclusion that in however strong a field, delocalized states with energy $\mathscr{E} \approx \mathscr{E}_{i,0}$ remain.

We shall consider one of the finite trajectories in real spae, connecting regions of mobile states. Since the potential fluctuation of all Landau levels is the same, this trajectory then corresponds to percolation equipotentials in each Landau subband. The carrier concentration in local regions of space along an equipotential line is constant; we shall denote it by n_{mob}. If N Landau levels are completely contained in the regions of space separated out by us, i.e.,

$$n_{\text{mob}} = N\mathscr{N}_H, \tag{8}$$

where

$$\mathscr{N}_H = He/ch, \tag{9}$$

then the charge transfer takes place without dissipation: $\rho_{xx} = \sigma_{xx} = 0$ ($\sigma_{ik} = \rho_{ik}^{-1}$ is the conductivity tensor).

Suppose the number of mobile carriers has changed insignificantly by an amount $\delta n_{\text{mob}} = n_{\text{mob}} - N\mathscr{N}_H \neq 0$. Then the mobile carriers have the possibility of dissipating energy; for small changes $\delta n_{\text{mob}} \ll \mathscr{N}_H$

$$\rho_{xx} \approx \sigma_{xx}/\sigma_{xy}^2 \propto |\delta n_{\text{mob}}|. \tag{10}$$

Since the whole current is only carried over regions of mobile states, while the localized states do not carry current, then[5]

$$\rho_{xy} = H/n_{\text{mob}}ec. \tag{11}$$

On taking Eq. (9) into account, the last equation agrees with Eq. (1) and the quantum Hall resistance is thus a consequence of the topology of the equipotentials of the 2D layer.[5,23] The localized states then act as a buffer separating equipotentials of mobile states in real space.

We see by varying Eq. (11) by δn_{mob} and comparing $\delta\rho_{xy}$ with Eq. (10) that our model achieves a linear relation between $\delta\rho_{xy}$ and ρ_{xx} in agreement with the experimental result.[6] We shall assume in what follows, in agreement with Eq. (11), that the small departures from Eqs. (1) and (2) are explained by a change in the concentration of mobile carriers along the percolation trajectories. The empirical result of Eq. (6) is an indication that the contribution to the current introduced by localized states can be neglected to a first approximation.

3.1.2 Width of the plateau for $T\rightarrow 0$, $J_x = 0$

1) The role of short-range fluctuations. Suppose that δ-shape fluctuations have a characteristic amplitude δU, characteristic radius $\mathscr{L}$ (where $\mathscr{L} < a_H$) and are distributed statistically uniformly over an area of the 2D layer with concentration N_δ. According to the Pauli principle, each of them can act as a localization center for one electron in the ith Landau level. The binding energy of such a state is

$$\mathscr{E}_b \approx \delta U \mathscr{L}^2/a_H^2 < \Gamma \ll \hbar\omega_c. \tag{12}$$

If we denote by $(1-\gamma)$ the fraction of the area free of long-range fluctuations, then the concentration of bound states determined by the δ-shaped fluctuations for each Landau subband is

$$\mathscr{N}_b' = (1-\gamma)\mathscr{N}_\delta. \tag{13}$$

2) The role of long-range fluctuations ($\mathscr{L} > a_H$). Each of

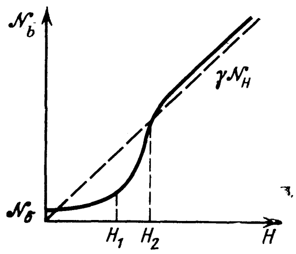

FIG. 6. Schematic dependence of the concentration $\mathscr{N}_b$ of bound states for $J_x = 0$ on magnetic field.

the long-range fluctuations produces a number $(\mathscr{L}/a_H)^2$ of bound states for each of the Landau sublevels. The number of bound states per unit area of the 2D layer is then

$$\mathscr{N}_b'' = \gamma \mathscr{N}_H, \tag{14}$$

where γ is the fraction of the area occupied by long-range fluctuations.

By summing the contributions of Eqs. (13) and (14) and taking into account the fact that for $T \to 0$ every quantum state with energy below $\mathscr{E}_F$ is filled, we obtain the total concentration of localized carriers for a Landau sublevel:

$$n_{\text{loc}} = \mathscr{N}_b = \gamma \mathscr{N}_H + (1-\gamma)\mathscr{N}_\delta, \tag{15}$$

i.e., the width of the plateau for $T \to 0$.

The parameter γ of Eqs. (13)–(15) is itself a function of magnetic field, so that our division of fluctuations into long-range and δ-shaped depends on the magnetic length $a_H \propto H^{-1/2}$. In a "weak" magnetic field ($a_H > \mathscr{L}_{\max}$) all fluctuations are δ-shaped and $\gamma = 0$ in Eq. (15). In the limit of high magnetic fields ($a_H < \mathscr{L}_{\min}$) all fluctuations become long-range and in Eq. (15) $\gamma = \gamma_0$, where $(1-\gamma_0)$ is the fraction of the area over which fluctuations do not exist at all. The magnetic field dependence of the concentration of localized carriers at $T = 0$ (i.e., the width of the plateau) should therefore be close to that shown in Fig. 6. The transition region is contained, as can be seen, between values of the magnetic field

$$H_1 = \hbar c/e\mathscr{L}^2_{max} \text{ and } H_2 = \hbar c/e\mathscr{L}^2_{min}.$$

Equation (15) is independent of the number l of the Landau levels, so that the magnetic radius occurs in it and not the cyclotron radius $r_H(l) = a_H(2l+1)^{1/2}$. This is a consequence of our assumption of the small energy $\mathscr{E}_b$ of the bound state.[12]

Discussion of Eq. (15)

1) The independence of n_{loc} of the number l in Eq. (15) agrees with experimental results shown in Table I, where the following symbols are used: N is the number of filled sublevels, l is the number of the highest filled Landau level, $\delta = |\delta\rho_{xy}|$ is the criterion of the deviation. Apart from these data, there are experiments[3,4] in which a narrowing of the plateau with increasing number l was observed, which the authors[4] approximate by an empirical dependence

$$\Delta n_{\text{plat}} \propto 1/r_H^2(l).$$

It must be borne in mind that Eq. (15) is only valid for $\Gamma \gg kT$, while this condition was not fulfilled in most experiments. The width of the plateau observed experimentally at finite T depends on Γ (see the results in §3.3.4.). The dependence of Γ on carrier concentration was in turn anomalously strong for specimens used by Kawaji and Wakabayashi[4] (the mobility changed 3.5-fold in the range of carrier concentrations studied).

2) In the field range $H_1 < H < H_2$ (see Fig. 6), Eq. (15) can be approximated by the expression $n_{\text{loc}} \approx A(H - H_0)$, which explains the linear dependence of the ρ_{xy} plateau width on H observed experimentally.[25–28] For a Si MIS, where screening is efficient, $\gamma < 1$, while for a GaAs heterojunction, where the screening radius is 12 times larger and when there is no metal gate, $\gamma \approx 1$. Equation (15) thus also explains the reason for wide plateaus in GaAs heterojunctions ($n_{\text{loc}} \approx 0.97\mathscr{N}_H$ for $T \to 0$, $J_x \to 0$, $H \to \infty$[27,28]) and narrower plateaus in Si MIS's ($n_{\text{loc}} \lesssim 0.5\mathscr{N}_H$ for $T \to 0$, $J_x \to 0$, $H \to \infty$.[10,25]) We note that if for $T \to 0$ the relation (4) $n_{\text{loc}} \propto H/l$ held in experiments,[27,28] then the plateau width should increase $\propto H^2$, which contradicts experimental results.[27,28]

3.2 Nonlinear phenomena in QHE. Percolation in the Hall field

3.2.1. Spatial distribution of Hall field

The qualitative discussion given above did not take into account the influence of Hall field E_y on carrier concentration in the 2D layer, so that it is only valid for infinitesimally small current J_x. It is necessary to know the distribution of current density j_x and of Hall field E_y over the width of the channel to find the influence of current on ρ_{xx} and ρ_{xy}.

We shall construct a qualitative field and current distribution, first of all considering a limiting case. We assume

TABLE I. Width of the plateau for different numbers of the Landau levels.

N	l	$\Delta n_{\text{plat}}/\mathscr{N}_H$		Experimental conditions	Source of data. Material measured
		$\delta=\pm 1\ \Omega$	$\delta=\pm 40\ \Omega$		
2	0	0,175	0,18	T=0,7 K,	Present work, Si
4	0	0.19	0,22	J_x=3 μA	MIS structure
8	1	0.18	0,21	H=80 kOe	with large channel
12	2		0,22		
4	0	0.28	0,45	T=0,4 K,	Present work, Si
8	1	0.28	0,42	J_x=1 μA	MIS structure
12	2	–	0,39	H=90 kOe	with small channel
2	0	–	0,5	T=1,5 K,	Ref. 1, Si MIS structure
4	0	–	0.5	H=180 kOe	
2	0	–	0,37	T=4,2 K,	Ref. 24, GaAs hetero-
4	1	–	0,37	H=32 kOe	junction with gate
6	2	–	0,39		

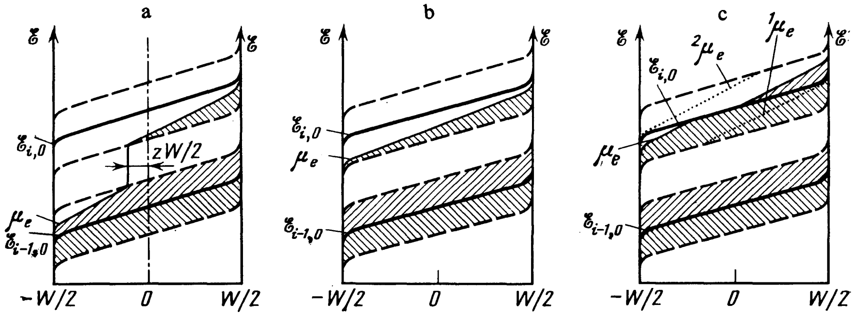

FIG. 7. Changes in the energy $\mathcal{E}_i$ of Landau subbands and of the electrochemical potential μ_e across the width of the channel: a) near the middle of the ρ_{xy} plateau and the ρ_{xx} minimum; b) in the region of wings of the ρ_{xy} plateau; c) in the region of the ρ_{xx} maximum, ${}^1\mu_e$ and ${}^2\mu_e$ are the limiting positions of the $\mu_e(y)$ curve, corresponding to the edges of the $\rho_{xx}(V_g)$ peak. The dashed lines respresent the nominal boundary of the Landau subband, where it is assumed that $D({}^{1,2}\mu_e \ll D(\mathcal{E}_{i,o})$. Different shading indicates the regions of bound states filled by electrons and holes respectively.

that the field is produced by a redistribution of mobile carriers, so that a surplus of electrons is accumulated on one side of the channel and of holes on the other. The image potential of the gate will screen the potential produced by the charged sides of the channel, as a result of which the Hall field decays even over a distance $\sim d_{SiO_2}$ from the side of the channel and over a large part of the cross section of the channel $E_y = 0$ and $j_x = 0$. Such a model, proposed by Halperin[29] from different considerations, agrees badly with the existence of QHE at large currents, since for a current flow of 10^{-6}–10^{-5} A, in two regions of width $\sim 10^{-5}$ cm the carrier drift velocity would be $\sim 10^7$ cm·s^{-1}, which is comparable with their Fermi velocity and is two orders of magnitude greater than the bulk velocity of sound.

An almost uniform distribution of current j_x and field E_y over the width of the channel with insignificant increases at the edges[30] seems more realistic to us (at least for current of 10^{-6}–10^{-5} A). These qualitative considerations are confirmed by calculations carried out[31] in the Hartree approximation. The energy of the conduction band, the valence band and the bottom of the potential well in this case change monotonically over the specimen width. The bottom of the electrical subband, just as the Landau levels, repeat this topography (Fig. 7) so that the total energy change of each Landau sublevel over the width of the channel is

$$\mathcal{E}_{i,0}(y=W/2)-\mathcal{E}_{i,0}(y=-W/2)=eV_y.$$

The distribution of carrier concentration in the 2D layer for $J_x \neq 0$

$$n(y)=\operatorname{div} E(y)/4\pi e$$

over the y coordinate is related self-consistently with the effective gate voltage $V_g^*(y)$, which changes from $V_g - V_y/2$ for $y = -W/2$ to $V_g + V_y/2$ for $y = +W/2$; the Fermi energy $\mathcal{E}_F \propto n \propto V_g$ also varies with the y coordinate correspondingly. For this reason the filling boundary of Landau levels with carriers, determined by the electrochemical potential

$$\mu_e=\mathcal{E}_F+U_H$$

(U_H is the Hall potential of the field), varies more rapidly with the y coordinate than the energy of the Landau levels (Fig. 7):

$$\frac{d\mu_e}{dy} \approx \frac{1}{W}\left[eV_y+\left(\frac{d\mathcal{E}_F}{dV_g}\right)V_y\right]. \qquad (16)$$

Three different cases for the position of the $\mu_e(y)$ line relative to the Landau level $\mathcal{E}_i$ are then possible.

1. The $\mu_e(y)$ line does not cross the $\mathcal{E}_{i,0}(y)$ line over the specimen width. In such a case current transport takes place over percolation trajectories below the level μ_e (in energy) and is not accompanied by dissipation. We consider a situation such that the $\mu_e(y)$ line passes simultaneously along a hole slope of the $i-1$ subband and an electron slope of the ith subband (Fig. 7,a); this corresponds to the middle of the ρ_{xy} plateau. Suppose that at some point y_0, $\mu_e(y)$ falls in the region of the energy gap between two neighboring Landau subbands. The density of states is small in this region, $(d\mathcal{E}_F/dV_g)_{y_0}$ increases sharply and according to Eq. (16) $d\mu_e/dy$ increases at the same time (see Fig. 7,a).

2. The $\mu_e(y)$ line does not cross the $\mathcal{E}_{i,0}(y)$ line and over all y passes over a region of only electron (or only hole) slope of one and the same Landau level. This situation corresponds to the electron (hole) wings of the ρ_{xy} plateau and is illustrated in Fig. 7,b.

3. The $\mu_e(y)$ line crosses the $\mathcal{E}_{i,0}(y)$ line at some point y_1. This case, illustrated in Fig. 7,c, corresponds to the appearance of a percolation trajectory at the level μ_e (i.e., dissipative current flow); the transition region between two neighboring ρ_{xy} plateaus and the ρ_{xx} maximum corresponds to it. On changing the gate voltage V_g (or the carrier concentration) the crossing point y_1 shifts along the channel width; the total width of the ρ_{xx} peak corresponds to a shift in y_1 over the range from $-W/2$ to $+W/2$ (Fig. 7,c). We note that by no means every crossing point of $\mu_e(y)$ with the level $\mathcal{E}_{i,0}$ belongs to a percolation trajectory, so that the appearance of a substructure to the $\rho_{xx}(V_g)$ peak similar to that observed[28] is possible.

The concentration of mobile carriers along the percolation trajectory can be calculated if the relative position of $\mu_e(y)$ and the energy level of the percolation equipotential $\mathcal{E}_{i,0}$ is known. According to Eq. (11) the behavior of ρ_{xy} for each of the three cases of Fig. 7 can then be described.

3.2.2. Shape of the ρ_{xy} plateau

The concentration of mobile carriers, averaged over the whole range of delocalized states at the percolation level $\mathcal{E}_{i-1,0}$ and $\mathcal{E}_{i,0}$ is

$$\frac{n_{\text{mob}}}{\mathcal{N}_H}=\frac{1}{W}\int_{-W/2}^{W/2}[f_F(\mathcal{E}_{i-1,0},\mu_e)+f_F(\mathcal{E}_{i,0},\mu_e)]\,dy. \qquad (17)$$

Here f_F is the Fermi distribution function. Integrating Eq. (17) near the center of the plateau $z\equiv[(V_g-{}^0V_g)/V_y]\ll 1$ gives[16]

$$\frac{\delta\rho_{xy}}{\rho_{xy}} = -\frac{\delta n_{\rm mob}}{N\mathcal{N}_H} \equiv -\frac{n_{\rm mob}-\mathcal{N}_H N}{N\mathcal{N}_H}$$

$$\approx \left(\frac{e^2}{h}\right)\frac{({}^0V_g-V_g)}{J_x}\left[e^{-\Gamma/kT}e^{\alpha}+e^{-(\hbar\omega_c-\Gamma)/kT}e^{-\alpha}\right], \qquad (18)$$

for large departures from the middle of the plateau $|z| \gg 1$

$$\left|\frac{\delta\rho_{xy}}{\rho_{xy}}\right| = \left|\frac{\delta n_{\rm mob}}{N\mathcal{N}_H}\right| \approx \frac{1}{2\alpha N}e^{-\Gamma/kT}e^{\alpha|z|}|e^{-\alpha}-e^{\alpha}|. \qquad (19)$$

In Eqs. (18) and (19) $\alpha = |(dn/dV_g)V_y/2D(\mu_e)kT|$ is the ratio of the number of carriers redistributed by the Hall field to the number of carriers in the energy band of width $2kT$.

Discussion of Eqs. (18) and (19)

Equation (18) agrees with recent measurements[32] in which the slope $\delta\rho_{xy}/dV_g$ in the central part of the plateau was shown with a temperature dependence $\propto \exp(\hbar\omega_c/(kT))$. Equation (18) describes the accuracy with which Eq. (1) is satisfied in an experiment for given $D(\mu_e)$, T, H and J_x. On the other hand, real values of the density of states $D(\mathcal{E})$ in the region of the wings of the Landau levels could be found from an experimental determination of the values of $d\rho_{xy}/dV_g$ for different V_y, T and H.

The exponential shape of the wings of the $\delta\rho_{xy}(V_g)$ plateau[16] agrees with Eq. (19) for large departures from the center of the $\delta\rho_{xy}(V_g)$ plateau. The exponent α of the exponential $\delta p_{xy}(V_g)$ dependence increases on lowering the temperature, which agrees with Eq. (19). The proportionality of the dependence of the exponent in Eq. (19) on current $\alpha \propto V_y \propto J_x$ also agrees with the empirical Eq. (5). Taking the linear relation of Eq. (6) into account, Eq. (19) also agrees with the exponential form of the ρ_{xx} minimum of Eq. (7) in Si MIS's and in GaAs heterojunctions.[25] However, according to Eq. (19), over a fairly wide intermediate region $V_y < |V_g - {}^0V_g| < 0.15$ V (or $|\delta\rho_{xy}/\rho_{xy}| = 10^{-3}$–$10^{-5}$, which does not agree with experiment) $\delta\rho_{xy} \propto \exp[A(V_g - {}^0V_g)/T]$. A similar disagreement has been found[10] in the activated temperature dependence and the reason for it is not clear.

3.2.3. Width of the ρ_{xy} plateau

In our model, the width of the plateau corresponds to the energy interval in which there are no infinite extended lines of $\mu_e(x,y)$ and $\mathcal{E}_{i,o}(x,y)$. We shall define the criterion for the width of the plateau at a given level of relative departure

$$\delta\rho_{xy}/\rho_{xy}=\pm\delta, \quad \text{i.e.} \quad \delta n_{\rm mob}/\mathcal{N}_H=\pm\delta, \qquad (20)$$

where the signs $\pm$ correspond to the electron and hole wings of the Landau level. By definition

$$\delta n_{\rm mob}=\mathcal{N}_H\int_{-W/2}^{W/2}[1-f_F(\mu_e(y),\mathcal{E}_{i,0}(y))]dy. \qquad (21)$$

We obtain the value $\mu_e^{\rm lim}$ from Eq. (21) determining the limit of the plateau according to the criterion δ. For the electron wing for $(V_g - {}^0V_g)/V_y > 1$ and neglecting transitions between Landau levels, i.e., for $\hbar\omega_c - 2\Gamma \gg T$

$$\mu_e^{\rm lim}(y=0)=\mathcal{E}_{i,0}-kT\ln\delta+2\alpha kT-kT\ln(2\alpha).$$

It follows from this that the plateau width on an energy scale is

$$\Delta\mathcal{E}_{\rm plat}=2[\Gamma-\mu_e^{\rm lim}(0)+\mathcal{E}_{i,0}]$$
$$=2[\Gamma-2kT\alpha+kT\ln\delta+kT\ln(2\alpha)]. \qquad (22)$$

Going over to a concentration scale, we have

$$\Delta n_{\rm plat}(T,J_x)\approx\Delta\mathcal{E}_{\rm plat}\left[D_b(\mu_e)+\frac{\pi^2}{6}(kT)^2D_b''(\mu_e)\right]. \qquad (23)$$

For example, for an elliptical density of states dependence at a Landau level

$$D_b(\mathcal{E})=\frac{\mathcal{N}_b}{2\Gamma}\left[1-\left(\frac{\mathcal{E}-\mathcal{E}_{i,0}}{\Gamma}\right)^2\right]$$

we obtain[16]

$$\Delta n_{\rm plat}\approx\Delta\mathcal{E}_{\rm plat}\frac{\mathcal{N}_b}{2\Gamma}\left[1-\frac{\pi^2}{3}\left(\frac{kT}{\Gamma}\right)^2-\left(\frac{\mu_e-\mathcal{E}_{i,0}}{\Gamma}\right)^2\right]. \qquad (24)$$

We note that the last equation is little sensitive to the actual form of the function $D_b(\mathcal{E})$.

Discussion of Eqs. (22) and (24)

1. Equation (24) is in qualitative agreement with experimental results[10] and in particular describes the reduction in the ρ_{xy} plateau width with increasing T and J_x. It also agrees with the linear current dependence of the width of the ρ_{xx} minimum which comes from experimental results.[25]

The "critical" current at which the temperature dependence $\Delta n_{\rm plat}(T)$ disappears is:

$$J^c=\left(\frac{Ne^2}{h}\right)\frac{\Gamma+kT\ln\delta}{(d\mu_e/dV_g)}. \qquad (25)$$

The critical temperature at which the current dependence $\Delta n_{\rm plat}(J_x)$ vanishes is:

$$T^c\leqslant 3^{1/2}\Gamma/\pi k. \qquad (26)$$

For evaluating T^c and J^c we put $(d\mu_e/dV_g)\sim\mathcal{E}_F/V_g$ and substitute into Eqs. (25) and (26) the values $\mathcal{E}_F/k = 70$ K, $V_g = 6$ V, $N = 4$, $\delta = 10^{-4}$ which are typical of an experiment.[10] To obtain $J^c = 15\ \mu$A [See Eq. (5)] it is then necessary to substitute $\Gamma/k = 10$ K into Eq. (25) and to obtain $T^c = 2.5$ K [Eq. (5)] requires substitution of $\Gamma/k \gtrsim 5$ K into Eq. (26). These values of Γ agree between themselves and with the estimate made earlier for the amplitude of potential fluctuations in an empty subband. The simple considerations given above cannot claim any rigour, since the dependence of screening radius on concentration and magnetic field [i.e., $\Gamma(V_g], H)$], possible current flow along the edges of the channel, a nonlinear $\mu_e(V_g)$ dependence and the real form of the density of states at the Landau level $D(\mathcal{E})$ were not taken into account.

Two departures of Eqs. (22) and (24) from the empirical Eq. (5) must be noted. First, in Eqs. (22) and (24) $d(\Delta n_{\rm plat})/d\ln\delta \propto kT$, while in Eq. (5) $d(\Delta n_{\rm plat})/d\ln\delta$ is independent of T. Secondly, the $\Delta n_{\rm plat}(T)$ dependence in Eq. (24) is close to quadratic, while it is linear in Eq. (5). The first disagreement can only be removed by assuming a temperature dependence

$$\delta n_{\text{mob}}/\mathcal{N}_H \propto \exp(BT) \tag{27}$$

instead of $\propto \exp(-A/T)$ (where A and B are independent of T). Equation (27) is remininiscent of the temperature dependent part of the Lifshitz-Kosevich formula for the amplitude of the de Haas-van Alphen effect. The second of the disagreements noted is less important and might disappear with a more realistic choice of the functions $\Gamma(V_g)$, $\mu_e(V_g)$ and $D(\mathscr{E})$.

2) Equations (22) and (24) also describe the dependence of plateau width on Γ. Assuming that Γ is related to the mobility μ (measured for $H=0$) by the equation[33]

$$\Gamma = \hbar\omega_c(2/\pi\mu H)^{1/2}, \tag{28}$$

we obtain from Eqs. (22) and (24) in the limit $kT \ll \Gamma$, the relation

$$\Delta n_{\text{plat}} \simeq \mathcal{N}_b \left(1 - \frac{kT\ln\delta}{\hbar\omega_c}\left(\frac{\pi\mu H}{2}\right)^{1/2}\right).$$

The last equation agrees qualitatively with the results of measurements,[21] where a narrowing of the plateau with increasing mobility μ was observed.

In deriving Eqs. (22) and (24) we neglected transitions between Landau levels, i.e., we considered $\hbar\omega_c - 2\Gamma \gg kT, \Gamma$. This condition may be destroyed on reducing the magnetic field and the wings of the levels may overlap. Dissipative conductivity $\sigma_{xx}^{\min}$ then grows appreciably leading to a narrowing of the ρ_{xy} plateau.

3.2.3. Percolation equipotentials in the Hall field

Until now, when considering the effect of the Hall field E_y, it has been assumed that the topology and structure of the percolation trajectories do not change when a field is applied. It is known that for a random potential the energy width of the band of percolation trajectories goes to 0 as $T \to 0$, and it is clear that a finite current cannot flow through a finite number of percolation trajectories for $T \to 0$. In other words, without a special choice of fluctuating potential $\delta U(x,y)$ in Eq. (15) the coefficient $(1-\gamma) \to 0$. It can be shown, however,[15,20] that for a random symmetric potential the band of percolation trajectories broadens in energy $\propto E_y$ for sufficiently small E_y; this is equivalent to the appearance of a relation $(1-\gamma) \propto E_y$ in Eq. (15). It is easy to understand this by considering an artifical potential of the "egg crate" type: $U(x,y) = U_0 \cos x \sin y$.

4. CONCLUSIONS

It has thus been shown in the present work that a study of nonlinear phenomena in the quantum Hall effect provides a large amount of experimental data for choosing and testing theoretical models which are indistinguishable in the linear approximation. We studied experimentally the shape of the ρ_{xx} minimum and of the wings of the ρ_{xy} plateau, and also the dependence of these quantities on the measuring current and temperature.

The main reason for the growth in ρ_{xx} and $|\delta\rho_{xy}|$, the change in mobile carrier concentration, can be derived from the linear relation found between ρ_{xx} and $\delta\rho_{xy}$ in the region of the wings of the ρ_{xy} plateau. This conclusion was used to find statistically the number of carriers in the case of a different relative position of the electrochemical potential and the mean energy of the Landau levels. As it turned out, the very simple theoretical model, developed above, provides a not bad explanation of most of the existing experimental data.

We limited the discussion to only the region of quantum magnetic fields where $N \gtrsim 1$. For $N \leqslant 1$ in the ultraquantum region, quantum effects play a special part and the quasiclassical approximation we used is inapplicable. In our view, to improve the agreement between theory and experiment, a subsequent self-consistent account must be taken of the screening of potential fluctuations by electrons and the current distribution over the channel (which we considered to be uniform) must be refined. An experimental elucidation of the current and field distribution over the width of the channel would be interesting, as would a more detailed experimental study of the effect of the potential variation in the 2D layer.

The authors are grateful to Yu. A. Bychkov, I. Ya. Krasnopolin, É. I. Rashba and D. E. Khmel'nitskiĭ for discussion of the results, and to A. S. Borovik-Romanov, M. S. Khaĭkin and V. S. Édel'man for their support of the present work.

[1)]Here "electrons" and "holes" at an electronic Landau level are in mind; these quasiparticles have the same effective mass and charges of opposite sign.

[1]K. V. Klitzing, G. Dorda, and M. Pepper, Phys. Rev. Lett. **45**, 494 (1980).
[2]K. V. Klitzing and G. Ebert, Physica (Utrecht) **117B–118B**, 682 (1983).
[3]K. Yoshihiro, J. Kinoshita, K. Inagaki, C. Yamanouchi, J. Moriyama, and S. Kawaji, Physica (Utrecht) **117B–118B**, 706 (1983); Surf. Sci. **113**, 16 (1982).
[4]S. Kawaji and J. Wakabayashi, Surf. Sci. **58**, 238 (1976).
[5]V. M. Pudalov and S. G. Semenchinskiĭ, Fiz. Khim. Mekh. **4**, 5 (1984).
[6]A. G. Eguiluz, A. A. Maradudin, and R. J. Elliott, Phys. Rev. B **27**, 4933 (1983).
[7]H. Fukuyama, P. M. Platzman, and P. W. Anderson, Surf. Sci. **73**, 374 (1978); Phys. Rev. B**19**, 5211 (1979).
[8]G. A. Baraff and D. C. Tsui, Phys. Rev. B **24**, 2274 (1981).
[9]R. J. Nicholas, R. A. Stradling, and R. J. Tidey, Solid State Commun. **23**, 341 (1977).
[10]V. M. Pudalov and S. G. Semenchinskiĭ, Pis'ma Zh. Eksp. Teor. Fiz. **37**, 474 (1983) [JETP Lett. **37**, 561 (1983)].
[11]F. Stern and W. E. Howard, Phys. Rev. **163**, 816 (1967).
[12]M. A. Vernikov, L. M. Pazinich, V. M. Pudalov, and S. G. Semenchinskiĭ, Pis'ma Zh. Tekh. Fiz. **8**, 820 (1982) [Sov. Tech. Phys. Lett. **8**, 355 (1982)].
[13]V. M. Pudalov and S. G. Semenchinskiĭ, Metrologia **4**, 37 (1983).
[14]R. J. Wagner, C. F. Lavine, M. E. Cage, R. F. Dziuba, and B. F. Field, Surf. Sci. **113**, 10 (1982).
[15]S. V. Iordansky, Solid State Commun. **43**, 1 (1982).
[16]V. M. Pudalov and S. G. Semenchinskiĭ, Pis'ma Zh. Eksp. Teor. Fiz. **38**, 173 (1983) [JETP Lett. **38**, 202 (1983)].
[17]T. Sugano, J. J. Chen, and T. Hamano, Surf. Sci. **98**, 154 (1980).
[18]B. I. Shklovskiĭ and A. L. Éfros, Electronic Properties of Doped Semiconductors [in Russian], Nauka, Moscow (1974).
[19]R. E. Prange and R. Joynt, Phys. Rev. B **25**, 2943 (1982).
[20]S. A. Trugman, Phys. Rev. B **27**, 7539 (1983).
[21]Y. Ono, J. Phys. Soc. Jpn. **51**, 237 (1982).
[22]H. Levine, S. B. Libby, and A. M. M. Pruiskin, Phys. Rev. Lett. **51**, 1915 (1983).
[23]R. F. Kazarinov and S. Luryi, Phys. Rev. B **25**, 7626 (1982); S. Luryi and R. F. Kazarinov, Phys. Rev. B **27**, 1386 (1983).
[24]S. Narita, S. Takeyama, W. B. Luo, S. Hiyamizu, K. Nambu, and H.

Hashimoto, Surf. Sci. **113**, 301 (1982).
[25]H. L. Stormer, D. C.Tsui, and A. C. Gossard, Surf. Sci. **113**, 32 (1982).
[26]S. Hiyamizu, K. Nambu, and H. Hasimoto, Surf. Sci. **113**, 301 (1982) [sicl.].
[27]M. A. Paalanen, D. C. Tsui, and A. C. Gossard, Phys. Rev. B **25**, 5566 (1982).
[28]G. Ebert, K. V. Klitzing, C. Probst, and K. Ploog, Solid State Commun. **44**, 95 (1982).
[29]B. I. Halperin, Phys. Rev. B **25**, 2185 (1982).
[30]R. E. Prange, Phys. Rev. B **23**, 4802 (1981).
[31]A. H. MacDonald, T. M. Rice, and W. F. Brinkman, Phys. Rev. B **28**, 3648 (1983).
[32]B. Tausendfreund and K. V. Klitzing, Surf. Sci. **142**, In Press.
[33]T. Ando, Y. Matsumoto, and Y. Uemura, J. Phys. Soc. Jpn. **39**, 279 (1975).

Translated by R. Berman